**RESEARCH ARTICLE**

# Unravelling the anti-inflammatory activity of *Cyperus rotundus* essential oil through gas chromatography-mass spectrometry analysis, network pharmacology and molecular docking approaches

Kendre Sandhya Rani[1], Ambika Sahoo[2], Sanghamitra Nayak[2], Pratap Chandra Panda[2], Monalisa Mohanty[1], Asit Ray[2]* & Sujata Mohanty[1]*

[1]P. G. Department of Biotechnology, Rama Devi Women's University, Bhubaneswar 751 002, Odisha, India

[2]Centre for Biotechnology, Siksha O Anusandhan (Deemed to Be University), Bhubaneswar 751 003, Odisha, India

[3]Agricultural Research, Education, and Extension Organization (AREEO), Karaj. 311-319

*Email: asitray2007@gmail.com, sujatamohanty@rdwu.ac.in

**OPEN ACCESS**

**Additional information**

**Reprints & permissions information** is available at https://horizonepublishing.com/journals/index.php/PST/open_access_policy

**Indexing**: Plant Science Today, published by Horizon e-Publishing Group, is covered by Scopus, Web of Science, BIOSIS Previews, Clarivate Analytics, NAAS, UGC Care, etc See https://horizonepublishing.com/journals/index.php/PST/indexing_abstracting

## Abstract

*Cyperus rotundus* rhizome is used in the traditional system of medicine to treat various diseases. The rhizomes of this plant are traditionally used as medicine for treatments of stomach pain, bowel disorders, and inflammatory pain. The present study aims to characterize the chemical constituents of the *C. rotundus* rhizomes essential oil (CREO) and to evaluate its possible mechanism of action as an anti-inflammatory agent by an integrative approach of gas chromatography-mass spectrometry (GC-MS), network pharmacology, and molecular docking analysis. The compound-target-disease network revealed cubenol, gamma murolene, cyperotundone, delta selinene, alpha copaene, alpha pinene, and beta caryophyllene are core compounds with higher degree values. Protein-protein interaction analysis revealed IL1B, IL10, IL6, PTGS2, TNF, and STAT3 as hub targets. A total of 1000 biological processes, 142 cellular components, and 241 molecular functional pathways were enriched. Molecular docking analysis revealed that hub compounds and protein targets had strong binding affinity between them. The top two docked poses with the lowest binding energy were identified as PTGS2-Cubenol and IL10-Gamma murolene with binding energies of -7.9 and -7.2 kcal/mol, respectively. A molecular dynamics study revealed that the PTGS2-Cubenol and IL10-Gamma murolene complex had a good amount of deformability. These results demonstrated that CREO can act on numerous proteins and pathways to form a systematic pharmacological network, and they can be considered as a candidate drug for treating inflammatory-related disorders.

## Keywords

GC MS; network pharmacology; molecular docking; *Cyperus rotundus*; anti-inflammatory activity

## Introduction

Inflammation is an immediate reaction caused by infectious microorganisms such as bacteria, viruses, and fungi entering the body. It is primarily a protective phenomenon characterized by heat, tumor, redness, and pain (1). Numerous inflammatory mediators are involved, which play an important role in the initiation, maintenance, and suppression of the process of inflammation (2). This biological process must be quick-acting to preserve the body's homeostasis; otherwise, it may cause different types of

immune related diseases (3). Numerous studies have attempted to correlate non-steroidal anti-inflammatory drugs (NSAID) and steroidal anti-inflammatory drugs (SAID) use with serious gastrointestinal, cardiovascular, and renal complications by determining the ratio of NSAID-related events with that of non NSAID-related events (4). Growing interest in the use of medicinal plants has come into existence for the treatment and control of different types of diseases related to inflammation. Therefore, it requires large efforts to identify more efficient and safer anti-inflammatory agents from plants rather than using synthetic drugs (5).

*C. rotundus,* commonly called nutsedge, belongs to the family Cyperaceae. It is a fibrous, rooted, perineal herb that reproduces widely through rhizomes and tubers. The rhizomes of *C. rotundus* are traditionally used as medicine for the treatment of stomach pain, bowel disorders, and inflammatory pain (6). Modern pharmacological studies showed that *C. rotundus* exhibits different properties such as anti-inflammatory, diuretic, antiperiodic, and treatment for diarrhoea, dysentery, bronchitis, blood disorders, and antipyretic activities. The essential oil obtained from *C. rotundus* rhizomes provides the characteristic odour and taste to the herb. It primarily consists of sesquiterpenes, including selinene, pinene, aristolone, cyperotundene, cypera2,4(15)-diene, caryophyllene, and other chemical compounds that are used for treating different diseases (6). Although the study has shown different properties of *C. rotundus* at present, there is no systematic analysis of its mechanism involved in treating inflammatory diseases.

Network pharmacology is a new generation analysis used to determine drug efficiency, based on the qualitative analysis that forms the compound-disease network. It is a challenging task to explain the mechanism of action of essential oils in the treatment of inflammation due to their complex mixture of several constituents, as the production of medicinal materials can vary based on the different growth environments, harvesting time, or other conditions that can affect the differences in the composition of medicinal materials within a plant (7). With the rapid progress in network pharmacology, the network-based drug-target discovery of traditional medicines is considered a promising approach toward the development and utilization of more efficient and safer drugs. By understanding the action targets of essential oils and anticipating their disease signalling pathways, several researchers have used network pharmacology as one of the standards in drug discovery.

Therefore, we used the method of network pharmacology to identify the potentially active compounds and therapeutic targets of inflammation to further analyse the mechanism of CREO in the treatment of inflammation. Molecular docking and simulation were carried out to study the interaction of potential compounds of CREO with anti-inflammatory targets.

## Materials and Methods

### Extraction of *C. rotundus* essential oil

Essential oil from *C. rotundus* was extracted by the hydro-distillation method using Clevenger apparatus. Essential oil content was determined on a fresh wt. basis oil content (%) = volume of essential oil (mL) / wt of fresh sample ×100. The component identification was achieved by the GC-MS analysis.

### Retrieval of chemical structure and evaluation of pharmacokinetics parameters

All the identified components of *C. rotundus* essential oil were chosen as targets. To acquire canonical SMILES for each compound, each compound was put into the PubChem database (https://pubchem.ncbi.nlm.nih.gov/) (7). The majority of the PubChem database is composed of three interlinked databases, *i.e.,* substance and compound bioassay. Descriptions uploaded by depositors make up the substance database. All the chemical structures extracted from the substance database were stored in the compound database. The bioassay database consists of all the results and descriptions of bioassay experiments (8).

A drug is effective only when its concentration to reach its target is sufficient. Development of a drug involves the assessment of adsorption, distribution, metabolism, and excretion (ADME). It can be done by using a web tool known as SwissADME (http://www.swissadme.ch/) (9). The drug likeness of each and every compound was calculated using Lipinski's rule of five through SwissADME software. For all the compounds selected, the parameters required to pass the drug likeness were: molecular weight <500, MlogP <5, hydrogen donors <5, hydrogen acceptors <10 and bioavailability >0.55. Highly active compounds were further analysed and the chemical structure of the compounds were collected (10).

### Mining of compound and anti-inflammatory gene targets

Swiss target prediction is a web server that allows us to identify the most probable macromolecular targets of small bioactive molecules (11) (http://www.swisstargetprediction.ch/). The canonical SMILES obtained were further input in the SwissTargetPrediction web server, and the species was selected as *Homo sapiens*. Then potential targets are identified using high-throughput screening. The repeating targets were removed, and the multiple isoforms were screened (12). A Comparative Toxicogenomics database (CTD) is a database that gives us information about the interaction between genes, drugs, and diseases (13). CTD helps in identifying cross species comparative studies of genes (http://ctdbase.org/). The target genes for the specific compounds can be retrieved using CTD. Therefore, these two databases, *i.e.,* SwissTargetPrediction and CTD, were used for the screening of targets (14).

Potential anti-inflammatory (AI)-related targets were obtained by using the keyword "Anti-inflammation'' as a query in different databases, such as Online Mendelian Inheritance in Man (OMIM) (https://www.omim.org/) and GeneCards (https://www.genecards.org/). These are

the databases that give us information on all the known and predicted genes for a particular disease (15). The Venny 2.1 software (https://bioinfogp.cnb.csic.es/tools/venny/) was used to obtain the overlapping genes from active compounds of *C. rotundus* essential oil and disease targets, *i.e.,* anti-inflammatory targets. There were 419 targets for *C. rotundus* essential oil (CREO) and 158 targets for Anti-inflammation (AI). After importing all the genes, we got 56 overlapping genes, which can be further used for constructing a protein-protein interaction network through Cytoscape 3.7.2 software (https://cytoscape.org/) (16).

### Protein-protein interactions analysis

The STRING (Search Tool for retrieval of interacting genes) is a database that systematically collects and integrates protein-protein interactions. The interaction obtained from this database includes both physical as well as functional associations. We uploaded the overlapping genes to the STRING database (https://string-db.org/), species were set as *Homo sapiens,* and the confidential score was set to be 0.7 to build a protein-protein interaction network. The results were imported to the network visualisation tool Cytoscape3.7.2 version in TSV format to further construct the PPI (protein-protein interaction) network and screening of hub genes based on degree, betweenness, and closeness. The nodes in the network represent the genes and edges represent the interactions among them (17).

### Gene ontology and pathway enrichment analysis

Gene ontology was performed on all the overlapping genes obtained to discover the role of these genes in molecular function, cellular components, and biological processes. The ShinyGO v0.741 web server (http://bioinformatics.sdstate.edu/go76/) was used to study the gene ontology (GO) and Kyoto Encyclopedia of Genes and Genomes (KEGG) enrichment analysis based on fold enrichment ratio (FDR<0.05) (18). A network was constructed using the ClueGO plugin in Cytoscape based on the pathways obtained from KEGG analysis to discover the target pathways involved in the anti-inflammatory effect of *C. rotundus* essential oil (19).

### Compound-Target Network construction

The compound target network was constructed using the CytoNCA plugin in Cytoscape based on all the active compound genes and disease gene targets. The genes were screened based on degree centrality, betweenness centrality, and closeness centrality. It was constructed to discover the relationship between active compounds of *C. rotundus* essential oil with that of gene targets of anti-inflammation (20).

### Molecular docking and molecular dynamic simulation

Molecular docking is a procedure for the virtual screening of small molecules and the prediction of compound-receptor complexes (21). It helps to discover new potential inhibitors against the target of interest. The top 8 compounds were selected with the highest degree from the compound-target network, and their 3D structures in SDF format are downloaded from the PubChem database (https://pubchem.ncbi.nlm.nih.gov/). Top 6 core targets with high degree were identified, and their relevant proteins in PDB format were obtained from the uniport database (https://www.rcsb.org/) (IL1B, PDB ID: 5R8Q), (IL10, PDB ID:2ILK), (TNF, PDB ID:2E7A), (IL6, PDB ID:1ALU), (PTGS2, PDB ID:5IKR), (STAT3, PDB ID:6NJS). By using BIOVIA discovery studio (https://discover.3ds.com/discovery-studio-visualizer-download) the proteins were refined by removing non-standard residues and water molecules to avoid clashes during the docking process (22).

By using PyRx software (https://pyrx.sourceforge.io/) all the docked ligands and their binding scores for each of the target proteins were discovered. The docking grid box was subsequently constructed in the AutoDock tool and then saved in PDBQT format. AutoDock Vina was used to conduct molecular docking among active compounds and core targets (23). The binding scores were calculated, and clusters having high binding affinity were selected *i.e.* PTGS2-Cubenol, IL10-Gamma muurolene, IL10-Delta selinene. Interactions between the active compounds and predicted proteins were further visualised using BIOVIA Discovery Studio (24). Molecular dynamic simulations of the complexes formed among protein-ligand were carried out using the iMOD server (http://imods.chaconlab.org/). Normal mode analysis is a tool used to study the functional motion of the macromolecules (25, 26). NMA is one of the most effective and natural approaches for modelling macromolecular conformational changes (27, 28). The docked PDB files obtained from docking analysis were uploaded to the iMOD server by setting all the parameters as default, and the stability of the protein-ligand complexes was represented with reference to their deformability, B-factor, eigenvalues, variance, covariance map, and elastic network (29).

## Results

### Chemical constituents of *C. rotundus* essential oil (CREO)

A total of 46 compounds were identified by gas chromatography and mass spectroscopy (GC-MS) analysis from *C. rotundus* essential oil. The compounds are listed based on their elution order on the Elite-5 MS column (Table 1). The essential oil was found to have the higher percentage of oxygenated sesquiterpene (58.39%) followed by sesquiterpene hydrocarbons (35.11%), monoterpene hydrocarbons (1.62%) and oxygenated monoterpenes (1.49%). Cyperene (13.26%), isolongifolen-5-one (10.24%), and spathulenol (6.99%) were the major constituents of *C. rotundus* essential oil.

**Table 1**. Chemical composition of *Cyperus rotundus* essential oil

| S. No | RI[a] | RI[b] | Compound | Area % |
|---|---|---|---|---|
| 1 | 930 | 939 | α-Pinene | 0.35±0.01 |
| 2 | 973 | 979 | β-Pinene | 1.27±0.03 |
| 3 | 1136 | 1139 | trans-Pinocarveol | 0.52±0.09 |
| 4 | 1190 | 1184 | Thujenal | 0.97±0.05 |
| 5 | 1355 | 1351 | α-Cubebene | 3.08±0.04 |

| 6 | 1368 | 1376 | α-Copaene | 4.84±0.07 |
|---|---|---|---|---|
| 7 | 1382 | 1390 | β-Elemene | 0.59±0.01 |
| 8 | 1394 | 1398 | Cyperene | 13.26±0.15 |
| 9 | 1438 | 1419 | β-Caryophyllene | 0.55±0.03 |
| 10 | 1452 | 1459 | Rotundene | 3.52±0.09 |
| 11 | 1463 | 1460 | allo-Aromadendrene | 1.27±0.07 |
| 12 | 1474 | 1477 | γ-Gurjunene | 0.86±0.04 |
| 13 | 1479 | 1477 | β-Chamigrene | 0.39±0.01 |
| 14 | 1482 | 1479 | γ-Muurolene | 1.26±0.07 |
| 15 | 1492 | 1482 | γ-Himachalene | 0.50±0.02 |
| 16 | 1508 | 1492 | δ-Selinene | 1.53±0.06 |
| 17 | 1511 | 1493 | cis-β-Guaiene | 0.41±0.01 |
| 18 | 1523 | 1512 | δ-Amorphene | 1.20±0.04 |
| 19 | 1531 | 1517 | α-dehydro-ar-Himachalene | 1.03±0.03 |
| 20 | 1541 | 1532 | (Z)-Nerolidol | 0.26±0.01 |
| 21 | 1555 | 1549 | Elemol | 0.71±0.02 |
| 22 | 1572 | 1578 | Spathulenol | 6.99±0.11 |
| 23 | 1579 | 1583 | Caryophyllene oxide | 0.72±0.04 |
| 24 | 1582 | 1590 | Globulol | 0.51±0.03 |
| 25 | 1584 | 1599 | Widdrol | 0.49±0.03 |
| 26 | 1586 | 1600 | Guaiol | 0.78±0.05 |
| 27 | 1599 | 1602 | Ledol | 3.29±0.07 |
| 28 | 1610 | 1607 | β-Biotone | 3.11±0.08 |
| 29 | 1617 | 1607 | β-Oplopenone | 0.65±0.02 |
| 30 | 1619 | 1608 | Humulene epoxide II | 0.49±0.03 |
| 31 | 1636 | 1641* | caryophylla-3,8(13)-dien-5-β-ol | 0.77±0.03 |
| 32 | 1647 | 1646 | Cubenol | 0.55±0.01 |
| 33 | 1650 | 1649* | caryophylla-3,8(13)-dien-5-α-ol | 0.82±0.01 |
| 34 | 1661 | 1651 | longiverbenone | 4.95±0.09 |
| 35 | 1674 | 1658 | Valerianol | 1.86±0.01 |
| 36 | 1679 | 1677 | Mustakone | 2.04±0.05 |
| 37 | 1685 | 1685 | Isolongifolen-5-one | 10.24±0.12 |
| 38 | 1698 | 1695 | Cyperotundone | 2.70±0.02 |
| 39 | 1702 | 1700 | Eudesm-7(11)-en-4-ol | 0.33±0.01 |
| 40 | 1717 | 1706* | Cyperenal | 1.02±0.06 |
| 41 | 1712 | 1727 | Valerenal | 1.28±0.06 |
| 42 | 1728 | 1743 | Aromadendrene epoxide | 0.27±0.04 |
| 43 | 1737 | 1746 | α-Cyperone | 2.85±0.03 |
| 44 | 1764 | 1763 | Aristolone | 6.98±0.10 |
| 45 | 1789 | 1806 | Nootkatone | 3.74±0.04 |
| 46 | 1904 | 1913 | 9,10-dehydro-Isolongifolene | 0.84±0.01 |
| Total identified | | | | 96.62±0.5 |
| Monoterpene hydrocarbons | | | | 1.62±0.06 |
| Oxygenated monoterpenes | | | | 1.49±0.14 |
| Sesquiterpene hydrocarbons | | | | 35.11±0.4 |
| Oxygenated sesquiterpenes | | | | 58.39±0.77 |

The values are represented as mean±SD (n=3). [a]RI calculated from homologous series of n-alkane ($C_8 – C_{20}$, $C_{21}$-$C_{40}$) on Elite-5 column. [b]RI from literature (Adams 2007).

## Screening of bioactive constituents, acquisition of compound and inflammation related targets

The compounds are further screened for drug-likeness based on Lipinski's rule using a SwissADME web tool. The screening was conducted based on different parameters such as molecular weight less than 500, hydrogen bond acceptors less than 10, hydrogen bond donors less than 5, and MLogP partition coefficient value less than 4.15. Abbott Bioavailability score should be greater than 0.1 standard value (Table 2). Out of 46 chemical constituents identified from GC-MS analysis, 44 were filtered out as bioactive constituents as they passed the above criteria.

The screened potentially active compounds were subjected to acquire the compound targets by mining several public databases. A total of 419 targets of active compounds were acquired from SwissTargetPrediction and Comparative Toxicogenomics Database. One hundred and fifty-eight disease targets of anti-inflammation were acquired from GeneCards and OMIM (Online Mendelian Inheritance in Man) databases. The overlapping targets of compound disease were obtained from the intersection of compound and disease target genes using the Venny 2.0 online tool. 56 common intersecting targets were obtained.

## Protein-protein interaction analysis of intersecting targets

All the overlapping targets were imported to the STRING database to build the protein-protein interaction (PPI) analysis. The species was selected as *Homo sapiens,* and the interaction score was set at 0.7 (highest confidence) for creating PPI analysis. The result obtained was saved in TSV format and was imported to Cytoscape for visualization. The PPI network consists of 41 nodes and 165 edges. The topological screening of protein-protein interaction analysis of the network was done using the CytoNCA plugin based on degree centrality. The top 6 proteins obtained after filtering were IL1B, IL10, IL6, PTGS2, TNF, and STAT3 (Fig. 1F).

## Compound target network analysis

To further clarify the relation between compounds and targets, a compound-target network was constructed using Cytoscape 3.7.2 version. The network consists of 104 nodes and 657 edges. Nodes represent the target genes and compounds; the edges represent the interaction between them, and the degree means the action intensity. Fig. 1(C) represents a compound target network. To detect potentially active compounds from the identified compounds, they were screened based on the degree of centrality. The 8 hub compounds cubenol (Degree:16), gamma-muurolene (Degree:16), cyperotundone (Degree:16), delta-selinene (Degree:16), alpha-copaene (Degree:16), alpha-pinene (Degree:17), beta-chamigrene (Degree:17), and beta-caryophyllene (Degree:33) obtained by degree filtering (degree >16) are shown in red color in Fig. 1(C).

## GO and KEGG pathway analysis

GO and KEGG pathway enrichment analysis was carried

**Table 2.** SwissADME analysis of active compounds

| S. No | Compound | MW<500 [g/mol] | MLOGP<5 | HBA<10 | HBD<5 | Lipinski violation | Drug like-liness |
|---|---|---|---|---|---|---|---|
| | | Lipinski rule of 5 | | | | | |
| 1 | α-Pinene | 136.23 | 4.29 | 0 | 0 | 1 | Pass |
| 2 | β-Pinene | 136.23 | 4.29 | 0 | 0 | 1 | Pass |
| 3 | trans-Pinocarveol | 152.23 | 2.3 | 1 | 1 | 0 | Pass |
| 4 | Thujenal | 164.24 | 2.49 | 1 | 0 | 0 | Pass |
| 5 | α-Cubebene | 204.35 | 5.65 | 0 | 0 | 1 | Pass |
| 6 | α-Copaene | 204.35 | 5.65 | 0 | 0 | 1 | pass |
| 7 | β-Elemene | 204.35 | 4.53 | 0 | 0 | 1 | Pass |
| 8 | Cyperene | 204.35 | 5.65 | 0 | 0 | 1 | Pass |
| 9 | β-Caryophyllene | 204.35 | 4.63 | 0 | 0 | 1 | Pass |
| 10 | Rotundene | 204.35 | 5.65 | 0 | 0 | 1 | Pass |
| 11 | allo-Aromadendrene | 204.35 | 5.65 | 0 | 0 | 1 | Pass |
| 12 | γ-Gurjunene | 204.35 | 4.63 | 0 | 0 | 1 | Pass |
| 13 | β-Chamigrene | 204.35 | 4.63 | 0 | 0 | 1 | Pass |
| 14 | γ-Muurolene | 204.35 | 4.63 | 0 | 0 | 1 | Pass |
| 15 | γ-Himachalene | 204.35 | 4.63 | 0 | 0 | 1 | Pass |
| 16 | δ-Selinene | 204.35 | 4.63 | 0 | 0 | 1 | Pass |
| 17 | cis-β-Guaiene | 204.35 | 4.63 | 0 | 0 | 1 | Pass |
| 18 | δ-Amorphene | 204.35 | 4.63 | 0 | 0 | 1 | Pass |
| 19 | α-dehydro-ar-Himachalene | 200.32 | 5.36 | 0 | 0 | 1 | Pass |
| 20 | (Z)-Nerolidol | 222.37 | 3.86 | 1 | 1 | 0 | Pass |
| 21 | Elemol | 222.37 | 3.56 | 1 | 1 | 0 | Pass |
| 22 | Spathulenol | 220.35 | 3.67 | 1 | 1 | 0 | Pass |
| 23 | Caryophyllene oxide | 220.35 | 3.67 | 1 | 0 | 0 | Pass |
| 24 | Globulol | 222.37 | 3.81 | 1 | 1 | 0 | Pass |
| 25 | Widdrol | 222.37 | 3.67 | 1 | 1 | 0 | Pass |
| 26 | Guaiol | 222.37 | 3.67 | 1 | 1 | 0 | Pass |
| 27 | Ledol | 222.37 | 3.81 | 1 | 1 | 0 | Pass |
| 28 | β-Oplopenone | 220.35 | 3.56 | 1 | 0 | 0 | Pass |
| 29 | Humulene epoxide II | 220.35 | 3.56 | 1 | 0 | 0 | Pass |
| 30 | Caryophylla-3,8(13)-dien-5-β-ol | 220.35 | 3.56 | 1 | 1 | 0 | Pass |
| 31 | Cubenol | 222.37 | 3.67 | 1 | 1 | 0 | Pass |
| 32 | Caryophylla-3,8(13)-dien-5-α-ol | 220.35 | 3.56 | 1 | 1 | 0 | Pass |
| 33 | longiverbenone | 218.33 | 3.56 | 1 | 0 | 0 | Pass |
| 34 | Valerianol | 222.37 | 3.67 | 1 | 1 | 0 | Pass |
| 35 | Mustakone | 218.33 | 3.56 | 1 | 0 | 0 | Pass |
| 36 | Isolongifolen-5-one | 218.33 | 3.56 | 1 | 0 | 0 | Pass |
| 37 | Cyperotundone | 218.33 | 3.56 | 1 | 0 | 0 | pass |
| 38 | Eudesm-7(11)-en-4-ol | 222.37 | 3.67 | 1 | 1 | 0 | Pass |
| 39 | Valerenal | 218.33 | 3.46 | 1 | 0 | 0 | Pass |
| 40 | Aromadendrene epoxide | 220.35 | 3.81 | 1 | 0 | 0 | Pass |
| 41 | α-Cyperone | 218.33 | 3.46 | 1 | 0 | 0 | Pass |
| 42 | Aristolone | 218.33 | 3.56 | 1 | 0 | 0 | Pass |
| 43 | Nootkatone | 218.33 | 3.46 | 1 | 0 | 0 | Pass |
| 44 | 9,10-dehydro-Isolongifolene | 200.32 | 4.93 | 0 | 0 | 1 | Pass |

**MW**-Molecular Weight, **HBA**- Hydrogen Bond Acceptor, **HBD**- Hydrogen Bond Donor and **MLogP**- Partition coefficient.
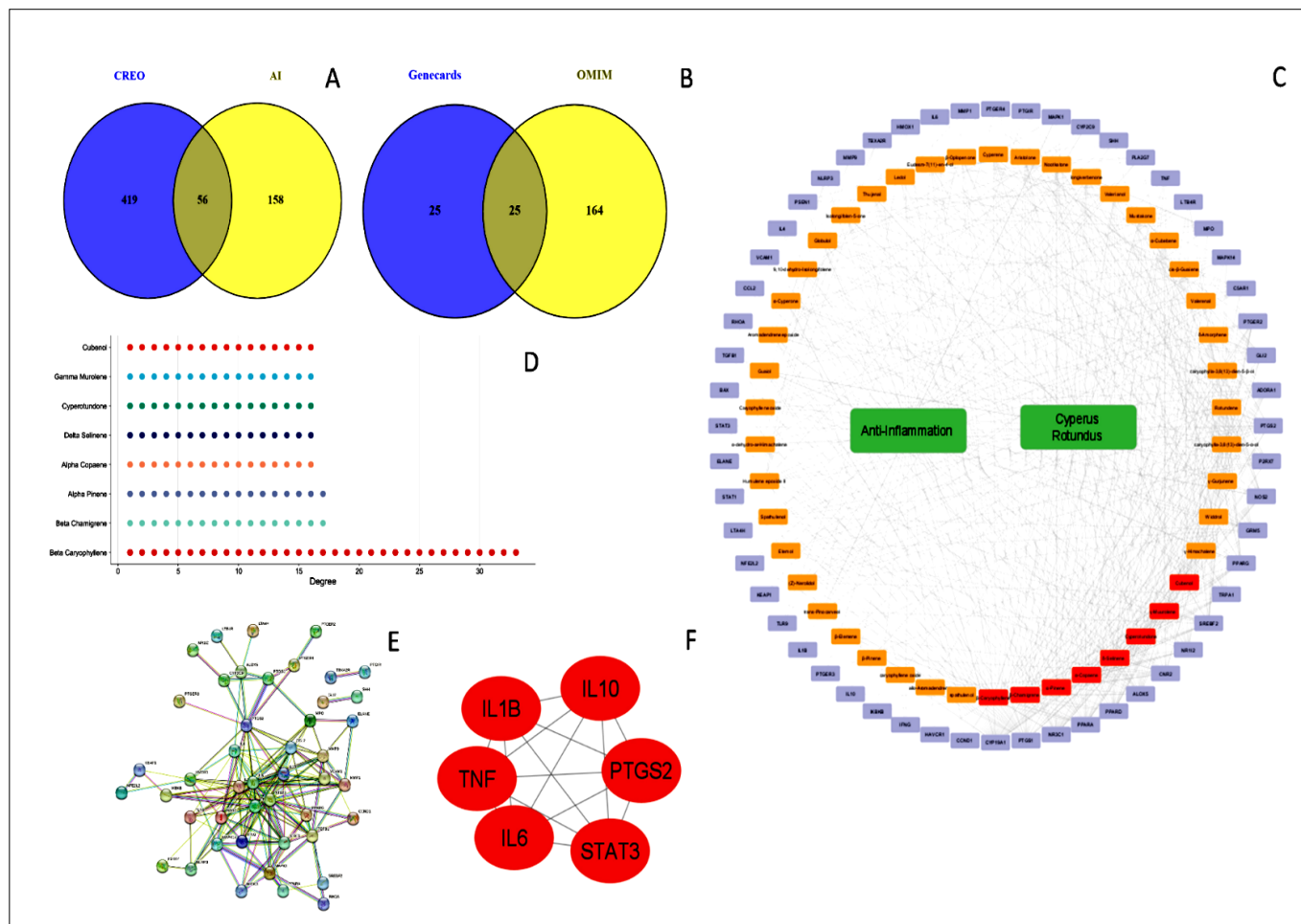
**Fig. 1**. Network pharmacology prediction of *Cyperus rotundus* essential oil in treatment of inflammation. (**A**) Venn diagram of overlapping targets of active compound genes (CREO) and anti-inflammatory (AI) targets. (**B**) Venn diagram of disease targets obtained from GeneCards and Online Mendelian Inheritance in Man (OMIM) databases. (**C**) Compound-Target network constructed using Cytoscape. The constituents of *C. rotundus* essential oil are shown in orange and target genes are shown in grey color. The hub compounds obtained by degree filtering using CytoNCA plugin of Cytoscape are shown in red. (**D**) Dot plot of hub compounds showing degree score constructed using SR plot. (**E**) Protein-protein interaction using STRING database. (**F**) Core genes obtained from protein-protein interactions using CytoNCA tool of Cytoscape.

out to understand the function and pathways of the isecting genes. GO enrichment analysis revealed that 1000 biological processes, 142 cellular components, and 241 mo-

lecular functions were involved in the treatment of inflammation. A bar chart was drawn to illustrate the top 10 enriched terms for each GO function in Fig. 2(A). The com-
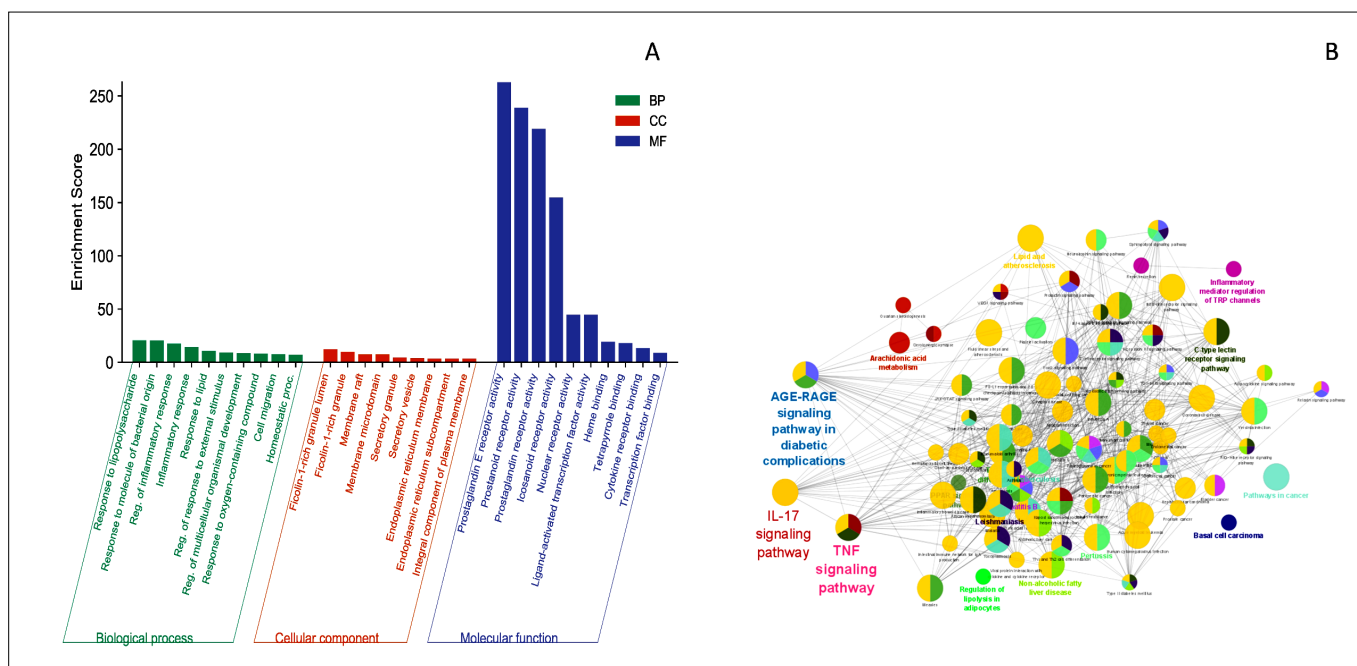


**Fig. 2.** Gene ontology (GO) and Kyoto Encyclopedia of genes and genomes (KEGG) enrichment analysis. (**A**) Top 10 GO terms (Biological process (BP), Cellular component (CC) and Molecular function (MF)) of the overlapping genes obtained from Venn diagram. The x-axis represents the enriched terms and the y-axis represents the enriched score. (**B**) KEGG pathway enrichment analysis of overlapping targets obtained using ClueGO plugin of Cytoscape.

mon targets regulate the inflammatory response, response to oxygen-containing compounds, regulation of response to external stimulus, response to lipids, homeostatic process, regulation of multicellular organismal development, response to lipopolysaccharide and cell migration through molecular functions like prostanoid, eicosanoid, prostaglandin and nuclear receptor activities, cytokine receptor binding, ligand-activated transcription factor activity, transcription factor binding, heme binding, prostaglandin E receptor activity, tetrapyrrole binding. The top 10 cellular components are the integral component of the plasma membrane, Secretory granule, intrinsic component of the plasma membrane, Membrane raft, Membrane microdomain, Ficolin-1-rich granule, Secretory vesicle, Ficolin-1-rich granule lumen, Endoplasmic reticulum membrane, endoplasmic reticulum sub compartment.

The dot plot diagram shown in Fig. 1(B) was used to represent the top 10 pathways linked to an inflammation based on their -logP value. The top 20 KEGG pathways with the highest enrichment ratio are shown below (Table 3). A network of these pathways was constructed using the ClueGO plugin of Cytoscape (Fig. 2B). The potential mechanism of *C. rotundus* essential oil in treating inflammation was mainly focused on the top 3 pathways, i.e., the IL17 signaling pathway, TNF signaling pathway, and AGE-RAGE signaling pathway. Inhibition of these pathways can be an excellent strategy to control inflammation.

## Molecular docking

Molecular docking was carried out to measure the binding affinity of active constituents of CREO and the hub target genes. 6 target proteins IL1B (PDB ID:5R8Q), IL10 (PDB ID:2ILK), TNF (PDB ID:2E7A), IL6 (PDB ID:1ALU), PTGS2 (PDB ID:5IKR), and STAT3 (PDB ID:6NJS) were docked with 8 active compounds having the highest degree, i.e., cubenol, gamma muurolene, cyperotundone, delta selinene, alpha copaene, alpha pinene, beta chamigrene, and beta caryophyllene. The Pyrx software was employed for molecular docking. Based on binding scores, a heat map analysis was carried out, which revealed the top three complexes with high binding affinity (Fig. 4A). The binding energies of PTGS2-cubenol, IL10-Gamma muurolene, and IL10-Delta selinene is -7.9, -7.2, and -7.2 kcal/mol, respectively. The 2D and 3D structural interactions of these three complexes are shown in Fig. 4B. The lower the binding energy, the stronger the interaction between them. The active compounds showing higher affinity towards the core targets help in the development of drugs and conducting further research. Cubenol showed the highest binding affinity with PTGS2 (-7.9 kcal/mol) by forming multiple interactions at binding sites, including vanderwaal, alkyl, and conventional hydrogen bond interactions. Similarly, gamma-muurolene displayed a binding energy of -7.2 kcal/mol with IL10 by forming multiple bindings with VAL33, MET77, LEU94, PHE37, VAL76, ALA80, TYR72, VAL91, and PHE80.

**Table 3**. KEGG pathway fold enrichment analysis

| S. No | Pathway | Enrichment FDR | Fold Enrichment | Genes |
|---|---|---|---|---|
| 1 | IL-17 signaling pathway | 7.71E-15 | 51.85 | PTGS2, MAPK1, MMP9, IKBKB, CCL2, IFNG, MAPK14, IL4, IL1B, IL6, MMP1. |
| 2 | Leishmaniasis | 3.84E-14 | 57.68 | NOS2, PTGS2, MAPK1, TGFB1, IFNG, MAPK14, IL4, STAT1, IL1B, IL10. |
| 3 | AGE-RAGE signalling pathway | 1.32E-14 | 48.22 | BAX, MAPK1, TGFB1, CCL2, CCND1, MAPK14, STAT1, IL1B, IL6, VCAM1, STAT3. |
| 4 | Malaria | 3.29E-12 | 71.57 | TGFB1, CCL2, IFNG, IL1B, IL6, IL10, VCAM1, TLR9. |
| 5 | Chagas disease | 1.32E-14 | 47.74 | NOS2, MAPK1, IKBKB, TGFB1, CCL2, IFNG, MAPK14, IL1B, IL6, IL10, TLR9. |
| 6 | Inflammatory bowel disease | 3.04E-11 | 53.95 | TGFB1, IFNG, IL4, STAT1, IL1B, IL6, IL10, STAT3. |
| 7 | C-type lectin receptor signaling pathway | 7.78E-13 | 42.15 | RHOA, PTGS2, MAPK1, IKBKB, MAPK14, STAT1, IL1B, IL6, IL10, NLRP3 |
| 8 | Lipid and atherosclerosis | 1.64E-18 | 32.77 | RHOA, BAX, MAPK1, MMP9, IKBKB, CCL2, MAPK14, NFE2L2, IL1B, PPARG, IL6, CYP2C9, VCAM1, NLRP3, STAT3, MMP1. |
| 9 | Th17 cell differentiation | 1.03E-12 | 40.59 | MAPK1, IKBKB, TGFB1, IFNG, MAPK14, IL4, STAT1, IL1B, IL6, STAT3. |
| 10 | African trypanosomiasis | 2.17E-09 | 71.09 | IFNG, IL1B, IL6, IL10, VCAM1, TLR9. |
| 11 | Pertussis | 8.51E-11 | 46.15 | NOS2, RHOA, MAPK1, MAPK14, IL1B, IL6, IL10, NLRP3. |
| 12 | TNF signaling pathway | 5.12E-11 | 35.22 | PTGS2, MAPK1, MMP9, IKBKB, CCL2, MAPK14, IL1B, IL6, VCAM1. |
| 13 | Toxoplasmosis | 5.12E-11 | 35.22 | NOS2, MAPK1, IKBKB, TGFB1, IFNG, MAPK14, STAT1, IL10, STAT3. |
| 14 | Fluid shear stress and athero-sclerosis | 1.04E-11 | 31.76 | RHOA, HMOX1, MMP9, IKBKB, CCL2, IFNG, MAPK14, NFE2L2, IL1B, VCAM1. |
| 15 | Tuberculosis | 1.54E-13 | 29.38 | NOS2, RHOA, BAX, MAPK1, TGFB1, IFNG, MAPK14, STAT1, IL1B, IL6, IL10, TLR9. |
| 16 | Pancreatic cancer | 3.53E-09 | 40.37 | BAX, MAPK1, IKBKB, TGFB1, CCND1, STAT1, STAT3. |
| 17 | Human cytomegalovirus infection | 4.56E-15 | 27.39 | PTGER3, RHOA, PTGS2, BAX, MAPK1, IKBKB, CCL2, CCND1, MAPK14, PTGER2, IL1B, IL6, STAT3, PTGER4. |
| 18 | Yersinia infection | 2.52E-10 | 28.79 | RHOA, MAPK1, IKBKB, CCL2, MAPK14, IL1B, IL6, IL10, NLRP3. |
| 19 | PD-L1 expression and PD-1 checkpoint pathway in cancer | 9.00E-09 | 34.47 | MAPK1, IKBKB, IFNG, MAPK14, STAT1, STAT3, TLR9. |
| 20 | Acute myeloid leukemia | 5.40E-08 | 39.25 | MPO, MAPK1, IKBKB, CCND1, PPARD, STAT3. |

**Table 4**. Binding energies of hub compounds with target proteins

| S. No | Compound | Protein | Binding energy |
|-------|----------|---------|----------------|
| 1 | Cubenol | | -5.5 |
| 2 | γ-Muurolene | | -5.5 |
| 3 | Cyperotundone | | -5.4 |
| 4 | δ-Selinene | IL1B | -5.8 |
| 5 | α-Copaene | (PDB: 5R8Q) | -5.4 |
| 6 | α-Pinene | | -4.6 |
| 7 | β-Chamigrene | | -5.5 |
| 8 | β-Caryophyllene | | -5.5 |
| 9 | Cubenol | | -6.6 |
| 10 | γ-Muurolene | | -7.2 |
| 11 | Cyperotundone | | -6.5 |
| 12 | δ-Selinene | IL10 | -7.1 |
| 13 | α-Copaene | (PDB: 2ILK) | -6.8 |
| 14 | α-Pinene | | -5.7 |
| 15 | β-Chamigrene | | -7.1 |
| 16 | β-Caryophyllene | | -7 |
| 17 | Cubenol | | -5.2 |
| 18 | γ-Muurolene | | -5.2 |
| 19 | Cyperotundone | | -5.4 |
| 20 | δ-Selinene | TNF | -5.4 |
| 21 | α-Copaene | (PDB: 2E7A) | -5.4 |
| 22 | α-Pinene | | -4 |
| 23 | β-Chamigrene | | -5.2 |
| 24 | β-Caryophyllene | | -5.2 |
| 25 | Cubenol | | -6.1 |
| 26 | γ-Muurolene | | -5.7 |
| 27 | Cyperotundone | | -5.8 |
| 28 | δ-Selinene | IL6 | -5.6 |
| 29 | α-Copaene | (PDB: 1ALU) | -5.9 |
| 30 | α-Pinene | | -5.3 |
| 31 | β-Chamigrene | | -5.8 |
| 32 | β-Caryophyllene | | -6.2 |
| 33 | Cubenol | | -7.9 |
| 34 | γ-Muurolene | | -6.5 |
| 35 | Cyperotundone | | -6 |
| 36 | δ-Selinene | PTGS2 | -6.7 |
| 37 | α-Copaene | (PDB: 5IKR) | -6.5 |
| 38 | α-Pinene | | -5.3 |
| 39 | β-Chamigrene | | -6.1 |
| 40 | β-Caryophyllene | | -6.2 |
| 41 | Cubenol | | -5.7 |
| 42 | γ-Muurolene | | -6 |
| 43 | Cyperotundone | | -5.4 |
| 44 | δ-Selinene | STAT3 | -6.1 |
| 45 | α-Copaene | (PDB: 6NJS) | -6.2 |
| 46 | α-Pinene | | -4.7 |
| 47 | β-Chamigrene | | -6 |
| 48 | β-Caryophyllene | | -5.7 |

## Molecular dynamic simulation analysis

Molecular dynamic simulations were employed using the iMOD server to assess the stability and physical moments of the docked complexes. The slow dynamics of the PTGS2-Cubenol and IL10-Gamma muurolene docked complexes were investigated, and their large-amplitude conformational variations were shown using normal mode analysis (NMA) (Fig. 5A, 6A). The peaks obtained from the deformability graph represent the regions in the protein with high deformability (Fig. 5B). Fig. 5C represents the B-Factor graph. The B-Factor also known as main-chain deformability, is a measure of a molecule's ability to deform at each of its residues. Fig. 5D represents the eigenvalue of the complex. The eigenvalue represents the motion stiffness associated with each normal mode. Its value is proportional to the amount of energy required to distort the structure. The lower the eigenvalue, the simpler is deformation. Fig. 5E represents the variance plot. The variance plot represents the individual variation, which is shown in purple-shaded bars, whereas the cumulative variation is shown in green-shaded bars. Fig. 5F represents a covariance map and demonstrates the correlation motion, uncorrelated motion, and anti-correlated motion between a pair of residues. Fig. 5G represents the elastic map of the docked complex. Each dot in the graph represents one spring inside the atoms' pair. The dots are colored depending on stiffness; the stiffer springs are indicated by darker grey dots and softer springs indicate lighter grey dots.

From the molecular dynamics study carried out, the PTGS2-Cubenol and IL10-Gamma muurolene complex revealed a good amount of deformability. Furthermore, the complex also showed a moderately low eigenvalue, suggesting that it could be deformed easily. The variance map exhibited a higher degree of cumulative variances as compared to individual variance. The satisfactory results have been observed through an elastic network.

## Discussion

Inflammation is a major driver causing multiple chronic diseases. Numerous studies show that uncontrolled inflammation may result in persistent tissue damage (30). Previously, researchers have attempted to correlate NSAID and SAID use with gastrointestinal, cardiovascular, and renal complications by determining the ratio of NSAID-related events with that of non-NSAID-related events (4). In present times, herbal remedies and dietary supplements have played a significant role in treating arthritis, rheumatic diseases, inflammatory bowel disease, and musculoskeletal and skin diseases (31). Ethnomedicinal claims revealed that the tubes of *C. rotundus* are used for treating dysmenorrheal, menstrual irregularities, pain, spasms, malaria, stomach disorders, and diarrhoea (32). Currently, there is no systematic analysis of its anti-inflammatory mechanism available. Therefore, in the current study, network pharmacology and molecular docking approaches were used to analyse the molecular mechanism of CREO in treating inflammation.

In this study, we have identified 46 compounds in
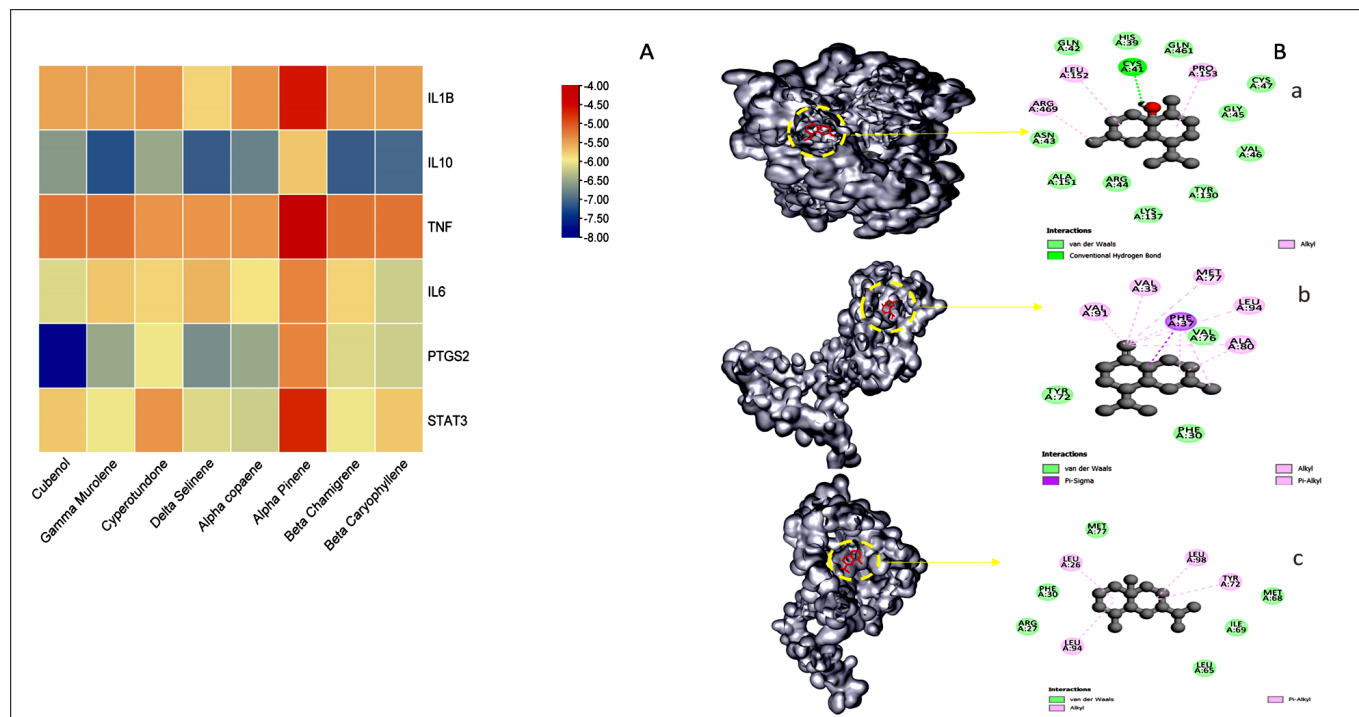
**Fig. 3.** Molecular docking analysis of hub compounds with target proteins (**A**) Heat map analysis of hub compounds and target genes based on binding energy scores. (**B**) 3D and 2D binding interaction plots of docking poses of top three compounds-protein targets (**a**) Cubenol-PTGS2 (**b**) Gamma Murolene-IL10 (**c**) Delta Selinene-IL10.
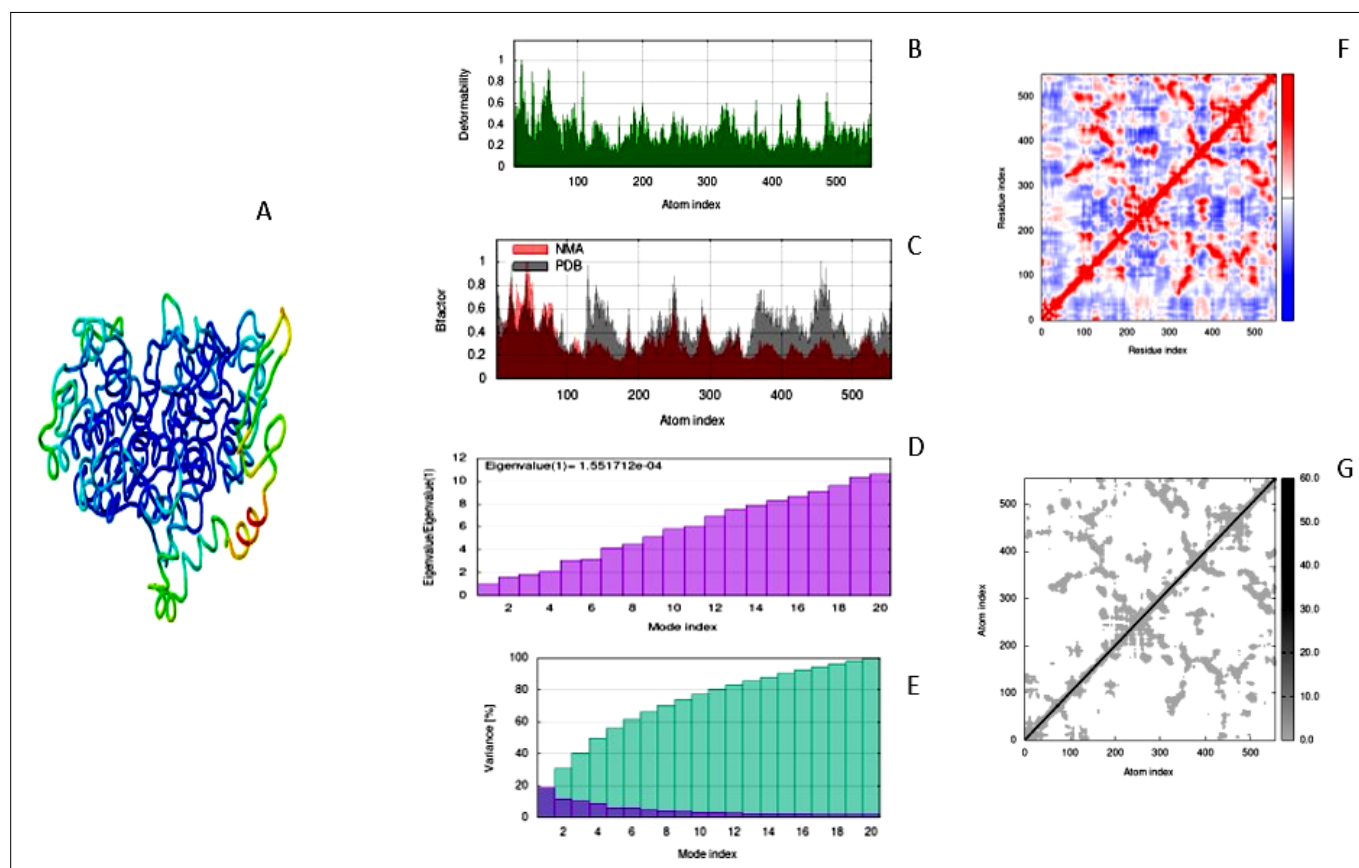


**Fig. 4.** Molecular dynamics simulation of PTGS2-Cubenol complex using iMODS server. (**A**) IL10 and Gamma-murolene docking complex. (**B**) Main chain deformability. (**C**) B-factor values. (**D**) Eigen value. (**E**) Variance. (**F**) Co-variance map. (**G**) Elastic network of model.

the *C. rotundus* essential oil, which mainly include oxygenated sesquiterpenes (58.39%) followed by sesquiterpene hydrocarbons (35.11%), monoterpene hydrocarbons (1.62%) and oxygenated monoterpenes (1.49%). A previous studies have reported that sesquiterpenes exert a wide range of biological and pharmacological activities, including anti-inflammatory, anti-cancerous, and anti-allergic (33, 34). Similarly, oxygenated sesquiterpenes are also known for their anti-bacterial activity against Gram-positive bacteria (35). It is very important to carry out pharmacokinetic screening of herbal medicine based on drug likeliness (Lipinski rule of five) and bioavailability score (36). A total of 44 active constituents were obtained after filtering the constituents based on drug-likeness and
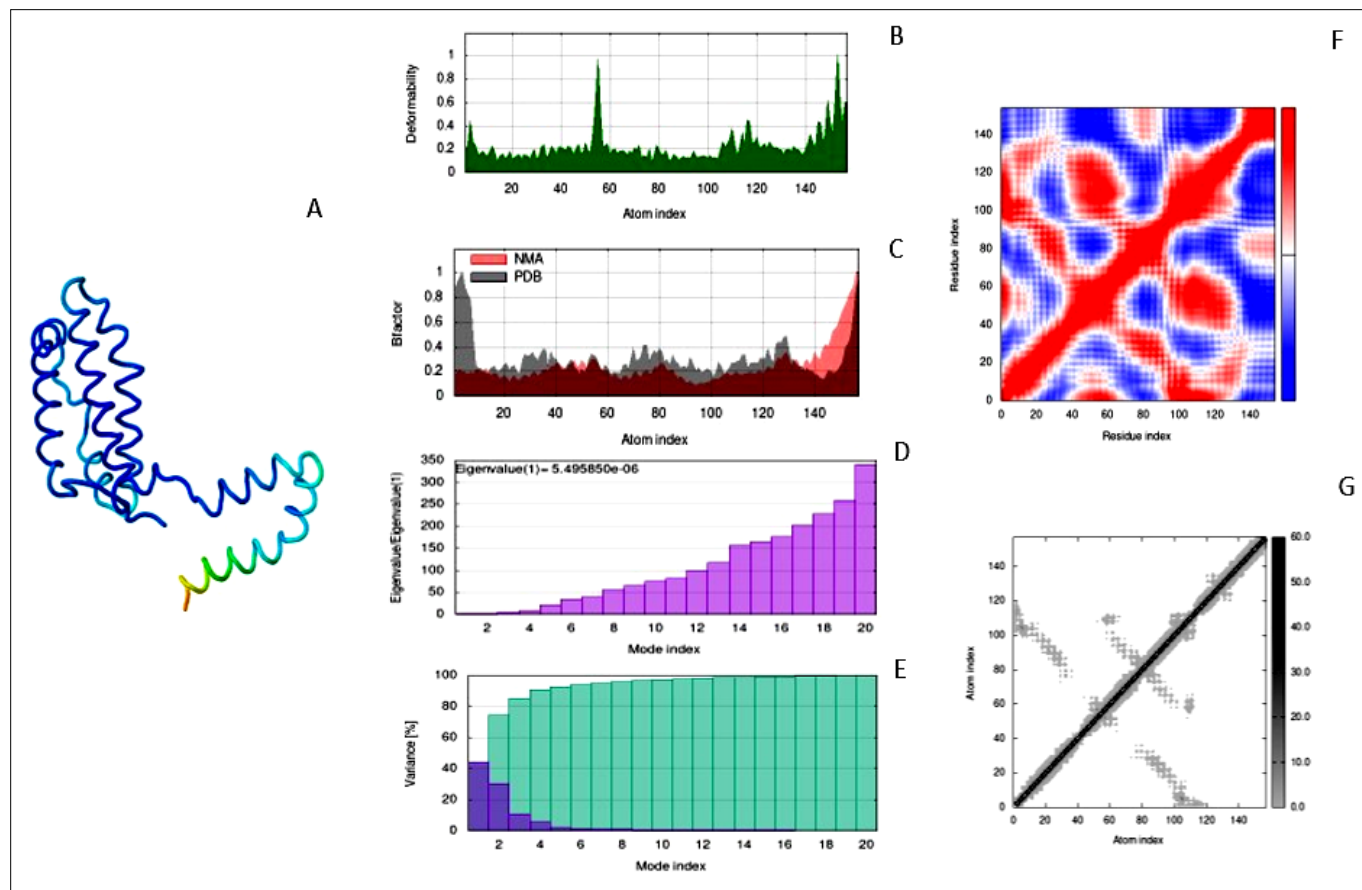
**Fig. 5.** Molecular dynamics simulation of IL10 and Gamma-murolene complex using iMODS server. (**A**) IL10 and Gamma-murolene docking complex. (**B**) Main chain deformability. (**C**) B-factor values. (**D**) The eigen value. (**E**) Variance. (**F**) Co-variance map. (**G**) Elastic network of model.

bioavailability score. Then, the compound-target network was constructed using Cytoscape software, which consists of 104 nodes and 657 edges. Based on degree filtering, cubenol (Degree:16), gamma-muurolene (Degree:16), cyperotundone (Degree:16), delta-selinene (Degree:16), alpha-copaene (Degree:16), alpha-pinene (Degree:17), beta-chamigrene (Degree:17), beta-caryophyllene (Degree:33) exhibited higher degree values than other compounds. Previous studies have shown the efficacy of beta-caryophyllene in wound healing and the treatment of different anti-inflammatory diseases (37, 38).

Inflammation disease targets were obtained from GeneCards and OMIM databases. The CREO and inflammation have 56 overlapping targets. These targets are considered potential targets of CREO in treating inflammation. Then, a protein-protein interaction network of overlapping targets was constructed using Cytoscape 3.7.2 software. Six genes, namely IL1B, IL10, IL6, PTGS2, TNF, and STAT3 with the highest degree, were identified. According to the previous study, IL1B activates inflammatory mediator cascades, and single nucleotide polymorphisms (SNPs) of IL1B promoters have been associated with different types of inflammatory diseases (39). IL10 plays an important role in downregulating pro-inflammatory cytokines and messenger RNA levels in Inflammatory Bowel Disease (IBD) patients (40). Studies have also shown that STAT3 has a potent anti-inflammatory role, which helps to regulate critical processes such as cell growth, apoptosis, and transcription of inflammatory genes (41). IL-6 is used to control inflammation levels in patients with cancer, bacterial in-

fection, or autoimmune diseases. It is also used as a biomarker for its role in activating and maintaining the inflammatory response (42). Vascular endothelial cells respond to TNF and undergo proinflammatory changes, which leads to an increase in leukocyte adhesion, transendothelial migration, and vascular leakage, leading to thrombosis (43). PTGS2 plays a crucial role in the regulation of inflammation and its inhibition may lead to reduced risk of colorectal cancer (44). From this, we can conclude that the hub genes obtained from network pharmacology analysis were closely related to inflammation.

GO and KEGG enrichment analysis was carried out using ShinyGO software. GO enrichment analysis revealed that the overlapping genes were involved in several biological processes such as inflammatory response, response to lipopolysaccharide, response to oxygen-containing compound, regulation of response to external stimulus, response to lipid, and homeostatic process. KEGG pathway enrichment analysis suggested that the IL17 signaling pathway, TNF signaling pathway, and AGE-RAGE signaling pathway are the key signaling pathways involved in the treatment of inflammation by CREO. As revealed from previous PPI analysis, 3 out of 6 core genes (IL1B, IL6, PTGS2) are involved in IL17 and TNF signaling pathways. Similarly, 3 out of 6 core genes (IL1B, IL6, and STAT3) are also involved in the AGE-RAGE signaling pathway. Previous studies suggest that the IL17 signaling pathway is an important pathway for targeted therapy of inflammatory diseases (45). The study shows IL-17 signalling pathway has been involved in the pathogenesis of multiple disorders includ-

ing cardiovascular and neurological diseases (46). TNF causes a huge range of pro-inflammatory alterations that boost vascular leak, transendothelial migration, leukocyte adhesion, and thrombosis. The capacity of TNF-blocking medications to treat a variety of inflammatory illnesses, such as rheumatoid arthritis, and inflammatory bowel disease, serves as evidence of TNF's essential involvement in inflammation (43). The AGE-RAGE pathway affects how the cells respond to cytokines, lipopolysaccharides, oxidised LDL, and glucose by converting a transient inflammatory response into a long-lasting alteration in cellular function that is increased by persistent activation of the proinflammatory transcription factor nuclear factor kappa-B (47).

To explore the potential mechanism of CREO in the treatment of inflammation based on the compound-target network and PPI analysis, core compounds were docked with hub genes. The docking results revealed that these core compounds had a strong interaction with hub genes. PTGS2-Cubenol and IL10-Gamma muurolene complex had the lowest binding energy. Although molecular docking is a quick and efficient approach to identifying the binding affinity of the ligand with that of the active site of the protein, it does not reveal the conformational changes that take place during protein-ligand interaction. To understand the deformability and mobility stiffness of PTGS2-Cubenol and IL10-Gamma muurolene complexes, normal mode analysis was carried out using the iMODS server. The iMODS analysis revealed that the complexes were stiff and had low deformability, with minimal differences observed in the flexibility and dynamics of protein and protein bound to ligands.

It should be mentioned that the present study had some limitations. Firstly, the results obtained from the research study were based on network pharmacology and molecular docking approach, which need to be verified further by carrying out pharmacodynamic and molecular biology experiments on animal models. Secondly, certain undetected compounds or targets might not be included in our analysis.

## Conclusion

In this study, network pharmacology and molecular docking were used to analyse the possible targets and the molecular mechanism of CREO in treating inflammation. In total, 8 active substances (Cubenol, gamma-muurolene, Cyperotundone, delta-selinene, alpha-copaene, alpha-pinene, beta-chamigrene, and beta-caryophyllene) and 6 possible target genes (IL1B, IL10, TNF, IL6, PTGS2, and STAT3) were screened based on high degree; these genes are mostly engaged in the IL17 signalling pathway, TNF signalling pathway, and the AGE-RAGE signalling pathway. By integrating literature research, network analysis, molecular docking, and molecular dynamic simulation analysis, our study provides a foundation for the mechanism and future research directions of CREO in treating inflammation.

## Authors' contributions

KSR drafted the manuscript. AS participated in data analysis.SN edited the manuscript. PCP participated in designing and coordination.MM performed statistical analysis. AR and SM participated in drafting, editing and data analysis. All authors read and approved the final manuscript.

## Compliance with ethical standards

**Conflict of interest**: Authors do not have any conflict of interests to declare.

**Ethical issues**: None

## References

1. Mohamed KA, Rajeshkumar S, Anjali AK. Antiinflammatory activity of silver nanoparticles synthesised using indian herbs -a review. Ann Rom Soc Cell Biol. 2021;25:5904-14. http://www.annalsofrscb.ro/index.php/journal/article/view/2125

2. Falcão HDS, Lima IO, Santos VLD, Dantas HDF, Diniz MDF, Barbosa-Filho JM, Batista LM. Review of the plants with anti-inflammatory activity studied in Brazil. Rev Bras Farmacogn. 2005;15:381-91. https://doi.org/10.1590/S0102-695X2005000400020

3. Tung YT, Chua MT, Wang SY, Chang ST. Anti-inflammation activities of essential oil and its constituents from indigenous cinnamon (*Cinnamomum osmophloeum*) twigs. Bioresour technol. 2008;99:3908-13. https://doi.org/10.1016/j.biortech.2007.07.050

4. Harirforoosh S, Asghar W, Jamali F. Adverse effects of nonsteroidal anti-inflammatory drugs: an update of gastrointestinal, cardiovascular and renal complications. J Pharm Pharm Sci. 2013;16:821-47. https://doi.org/10.18433/J3VW2F

5. Obaidullah AJ, Alanazi MM, Alsaif NA, Alanazi AS, Albassam H, Az A, et al . Network pharmacology and molecular docking-based identification of potential phytocompounds from *Argyreia capitiformis* in the treatment of inflammation. Evidence-Based Complementary and Alternative Medicine. 2022;2022:22. https://doi.org/10.1155/2022/8037488

6. Meena AK, Yadav AK, Niranjan US, Singh B, Nagariya AK, Verma M. Review on *Cyperus rotundus*-a potential herb. Int J Pharm Clin Res. 2010;2:20-22.

7. Wang Y, Zou J, Jia Y, Zhang X, Wang C, Shi Y, et al. The mechanism of lavender essential oil in the treatment of acute colitis based on "Quantity-Effect" weight coefficient network pharmacology. Front Pharmacol. 2021;12. https://doi.org/10.3389/fphar.2021.644140

8. Kim S, Chen J, Cheng T, Gindulyte A, He J, He S, et al. Improved access to chemical data. PubChem Nucleic Acids Res. 2019; 47:D1102-D1109. https://doi.org/10.1093/nar/gky1033

9. Daina A, Michielin O, Zoete V. SwissADME: a free web tool to evaluate pharmacokinetics, drug-likeness and medicinal chemistry friendliness of small molecules. Sci Rep. 2017;7:42717. https://doi.org/10.1038/srep42717

10. de Moraes ÂAB, Cascaes MM, do Nascimento LD, de Jesus PFC, Ferreira OO. Chemical evaluation, Phytotoxic Potential and *In silico* study of essential oils from leaves of *Guattera schomburgkiana* Mart. and *Xylopia frutescens* Aubl.

(Annonaceae) from the Brazilian Amazon. Molecules. 2023;28:2633. https://doi.org/10.3390/molecules28062633

11. Gfeller D, Grosdidier A, Wirth M, Daina A, Michielin O, Zoete V. SwissTargetPrediction: a web server for target prediction of bioactive small molecules. Nucleic Acids Res. 2014;42:W32-38. https://doi.org/10.1093/nar/gku293

12. Zhang Q, Liu J, Li R, Zhao R, Zhang M, Wei S, et al. A network pharmacology approach to investigate the anticancer mechanism and potential active ingredients of *Rheum palmatum* L. against lung cancer via induction of apoptosis. Front Pharmacol. 2020;11:528308. https://doi.org/10.3389/fphar.2020.528308

13. Mattingly CJ, Rosenstein MC, Colby GT, Forrest Jr JN, Boyer JL. The Comparative Toxicogenomics Database (CTD): a resource for comparative toxicological studies. J Exp Zool A Comp Exp Biol. 2006;305:689-92. https://doi.org/10.1002/jez.a.307

14. Guan M, Guo L, Ma H, Wu H, Fan X. Network pharmacology and molecular docking suggest the mechanism for biological activity of rosmarinic acid. Evidence-Based Complementary and Alternative Medicine. 2021.p.1-10. https://doi.org/10.1155/2021/5190808

15. Deng H, Jiang J, Zhang S, Wu L, Zhang Q, Sun W. Network pharmacology and experimental validation to identify the potential mechanism of *Hedyotis diffusa* Willd against rheumatoid arthritis. Sci Rep. 2023;13:1425. https://doi.org/10.1038/s41598-022-25579-3

16. Xiao G, Zeng Z, Jiang J, Xu A, Li S, Li Y, et al. Network pharmacology analysis and experimental validation to explore the mechanism of Bushao Tiaozhi capsule (BSTZC) on hyperlipidemia. Sci Rep. 2022;12:6992. https://doi.org/10.1038/s41598-022-11139-2

17. Szklarczyk D, Gable AL, Lyon D, Junge A, Wyder S, Huerta CJ, et al . STRING v11: protein –protein association networks with increased coverage, supporting functional discovery in genome wide experimental datasets. Nucleic Acids Res. 2019;47:D607-13. https://doi.org/10.1093/nar/gky1131

18. Nandi A, Das A, Dey YN, Roy KK. The abundant phytocannabinoids in rheumatoid arthritis: therapeutic targets and molecular processes identified using integrated bioinformatics and network pharmacology. *Life.* 2023;*13:*700. https://doi.org/10.3390/life13030700

19. Ijaz M, Huang X, Buabeid M, Chohan TA, Murtaza G, Shamim S. Mechanistic investigation of *Glycyrrhiza uralensis* effects against respiratory ailments: application of network pharmacology and molecular docking approaches. Lett Drug Des Discov. 2022;19:397-412. https://doi.org/10. 2174/1570180818666211119113853

20. Tang Y, Li M, Wang J, Pan Y, Wu FX. CytoNCA: a cytoscape plugin for centrality analysis and evaluation of protein interaction networks. Biosyst. 2015;127:67-72. https://doi.org/10.1016/j.biosystems.2014.11.005

21. Dias R, de Azevedo J, Walter F. Molecular docking algorithms. Curr Drug Targets. 2008;9:1040-47. https://doi.org/10.2174/138945008786949432

22. Noor F, Rehman A, Ashfaq UA, Saleem MH, Okla MK, Al-Hashimi A, et al. Integrating network pharmacology and molecular docking approaches to decipher the multi-target pharmacological mechanism of *Abrus precatorius* L. acting on diabetes. *Pharm*. 2022;*15:*414. https://doi.org/10.3390/ph15040414

23. Muhammad SA, Fatima N. *In silico* analysis and molecular docking studies of potential angiotensin-converting enzyme inhibitor using quercetin glycosides. Pharmacogn Mag. 2015;1:S123-26. https://doi.org/10.4103%2F0973-1296.157712

24. Dallakyan S, lson AJ. Small-molecule library screening by docking with PyRx. Chemical Biology Methods and Protocols. 2015. p. 243-50.

25. Bahar I, Rader AJ. Coarse-grained normal mode analysis in structural biology. Curr Opin Struct Biol. 2005;15:586-92. https://doi.org/10.1016/j.sbi.2005.08.007

26. Dykeman EC, Sankey OF. Normal mode analysis and applications in biological physics. J Phys Condens Matter. 2010;22:423202. https://doi.org/10.1088/0953-8984/22/42/423202

27. Ma J. Usefulness and limitations of normal mode analysis in modeling dynamics of biomolecular complexes. Structure. 2005;13:373-80.

28. López-Blanco JR, Aliaga JI, Quintana-Ortí ES, Chacón P. iMODS: internal coordinates normal mode analysis server. Nucleic Acids Res. 2014;42:W271-76. https://doi.org/10.1093/nar/gku339

29. Sumera, Anwer F, Waseem M, Fatima A, Malik N, Ali A, Zahid S. Molecular docking and molecular dynamics studies reveal secretory proteins as novel targets of temozolomide in glioblastoma multiforme. *Molecules*. 2022; *27:*7198. https://doi.org/10.3390/molecules27217198

30. Nathan C, Ding A. Nonresolving inflammation. Cell. 2010;140:871-82.

31. Mobasheri A. Intersection of inflammation and herbal medicine in the treatment of osteoarthritis. Curr Rheumatol Rep. 2012;14:604-16. https://doi.org/10.1007/s11926-012-0288-9

32. Zhu M, Luk HH, Fung HS, Luk CT. Cytoprotective effects of *C. rotundus* against ethanol induced gastric ulceration in rats. Phytotherapy Res. 199711:392-94. https://doi.org/10.1002/(SICI)1099-1573(199708)11:5%3C392::AID-PTR113%3E3.0.CO;2-1

33. Jin JH, Lee DU, Kim YS, Kim HP. Anti-allergic activity of sesquiterpenes from the rhizomes of *Cyperus rotundus*. Arch Pharmacal *Res*. 2011;34: 223-28. https://doi.org/10.1007/s12272-011-0207-z

34. de Cássia DSR, Andrade LN, De Sousa DP. Sesquiterpenes from essential oils and anti-inflammatory activity. Nat Prod Com. 2015;10:1767-74.

35. Kilani S, Abdelwahed A, Ammar RB, Hayder N, Ghedira K, Chraief I, et al. Chemical composition, antibacterial and antimutagenic activities of essential oil from (Tunisian) *Cyperus rotundus*. J Essent Oil Res. 2005;17:695-700. https://doi.org/10.1080/10412905.2005.9699035

36. Zhang MQ, Wilkinson B. Drug discovery beyond the 'rule-of-five'. Curr Opin Biotechnol. 2007;18:478-88. https://doi.org/10.1016/j.copbio.2007.10.005

37. Koyama S, Purk A, Kaur M, Soini HA, Novotny MV, Davis K, et al. Beta-caryophyllene enhances wound healing through multiple routes. PloS One. 2019;14:e0216104. https://doi.org/10.1371/journal.pone.0216104

38. Gushiken LFS, Beserra FP, Hussni MF, Gonzaga MT, Ribeiro VP, et al. Beta-caryophyllene as an antioxidant, anti-inflammatory and re-epithelialization activities in a rat skin wound excision model. Oxid *Med Cell Longev.* 2022;2022:9004014. https://doi.org/10.1155/2022/9004014

39. Rogus J, Beck JD, Offenbacher S, Huttner K, Iacoviello L, Latella MC, et al. IL1B gene promoter haplotype pairs predict clinical levels of interleukin-1β and C-reactive protein. Hum Genet. 2008;123:387-98. https://doi.org/10.1007/s00439-008-0488-6

40. Schreiber S, Heinig T, Thiele HG, Raedler A. Immunoregulatory role of interleukin 10 in patients with inflammatory bowel disease. Gastroenterol. 1995;108:1434-44. https://doi.org/10.1016/0016-5085(95)90692-4

41. Egwuagu CE. STAT3 in CD4+ T helper cell differentiation and inflammatory diseases. Cytokine. 2009;47:149-56. https://doi.org/10.1016/j.cyto.2009.07.003

42. Kany S, Vollrath JT, Relja B. Cytokines in inflammatory disease. Int J Mol Sci. 2019;20:6008. https://doi.org/10.3390/ijms20236008

43. Bradley J. TNF-mediated inflammatory disease. The Journal of Pathology: A Journal of the Pathological Society of Great Britain and Ireland. 2008;214:149-60. https://doi.org/10.1002/path.2287

44. Ulrich CM, Whitton J, Yu JH, Sibert J, Sparks R, Potter JD, Bigler J. PTGS2 (COX-2) −765G> C promoter variant reduces risk of colorectal adenoma among nonusers of nonsteroidal anti-inflammatory drugs. Cancer Epidemiology Biomarkers and Prevention. 2005;14:616-19. https://doi.org/10.1158/1055-9965.EPI-04-0510

45. Tulotta C, Ottewell P. The role of IL-1B in breast cancer bone metastasis. Endocr Relat Cancer. 2018;25:R421-34. https://doi.org/10.1530/ERC-17-0309

46. Mills KHG. IL-17 and IL-17-producing cells in protection versus pathology. *Nat Rev Immunol.* 2023;23:38-54. https://doi.org/10.1038/s41577-022-00746-9

47. Bierhaus A, Nawroth PP. Multiple levels of regulation determine the role of the receptor for AGE (RAGE) as common soil in inflammation, immune responses and diabetes mellitus and its complications. Diabetologia. 2009;52:2251-63. https://doi.org/10.1007/s00125-009-1458-9.